Proceedings of the Twenty-first (2011) International Offshore and Polar Engineering Conference
Maui, Hawaii, USA, June 19-24, 2011

ISBN 978-1-880653-96-8 (Set); ISSN 1098-6189 (Set); www.isope.org

The Thermal Ice Melt Feedback Mechanism of Near Sea-surface Temperature Maximum

Yong Cao[1], Jinping Zhao[1],Zhihua Chen[2]
1. The Key Laboratory of Physical Oceanography, Ocean University of China, Qingdao, China
2. Bengbu Muyuan School, Anhui, China

ABSTRACT

Near Sea-surface Temperature Maximum (NSTM) appears at the depth less than 40m in the Arctic sea ice covered region. The solar radiation is the direct heating source of NSTM. Although most of the solar radiation is reflected back into the atmosphere by the sea ice, part of it is absorbed by the sea ice, and the rest heats the surface sea water by penetrating through the sea ice. However, most of this heat diffuses back upwards due to the existence of pycnocline forming a temperature peak (NSTM) just above it. By heating the water below the sea ice, the heat from the NSTM will accelerate the melting of sea ice. This is the thermal feedback mechanism of NSTM.
A thermodynamic coupled sea ice-upper ocean column model was used in this paper to examine the relationship between the solar radiation flux penetrating through the sea ice and maximum temperature of NSTM. When the vertical eddy diffusivity was fixed as 1.0e-6m^2s^{-1}, the solar energy through the sea ice ranged from 10.90Wm^{-2} to 45.30 Wm^{-2} corresponding the maximum temperature range from -1.23^oC to -0.39^oC. The energy of sea ice obtained from NSTM was calculated also. The heat flux absorbed by the sea ice bottom was from 5.64 Wm^{-2} to 23.31 Wm^{-2}.

KEY WORDS: Arctic; Canada Basin; Sea ice; Near Sea-surface Temperature Maximum.

1. INTRODUCTION

The Near Sea-surface Temperature Maximum (NSTM) is a distinct layer separated from the deeper temperature maxima, which is defined as having a salinity less than 31 and the maximum temperature is at least 0.2^oC above the freezing temperature (Jackson et al., 2010). The solar radiation penetrating through sea ice is the energy source for the NSTM (Maykut and McPhee, 1995; Kadko, 2000; Zhao et al., 2003; Chen et al., 2010; Jackson et al., 2010). And the surface cooling is another basic mechanism to form the NSTM in the water under sea ice (Zhao et al., 2003). In summer, the NSTM occurred frequently in Arctic since 2003 and is thought to be related with the sea ice rapid change in the sea ice concentration (Cao et al., 2010).
Maykut and Untersteiner (1971) used a sea ice thermodynamic column model (MU model) to model the time-dependent vertical diffusion process. The Mu model included the effects of internal heating due to penetrating solar radiation and the internal storage of heat in brine pockets, and allowed variation of the specific heat and thermal conductivity of ice with temperature. Semtner (1976) simplified the MU model, such as improved the difference scheme, simplified the diffusion equations and reduced the layers from 40 to 3. The results of this model were similar to the MU model. In terms of sea–air interaction Ebert and Curry (1993) developed a better three-dimensional ice thermodynamic model based on the MU model. In this model leads and meltwater ponds were considered and the surface albedo was improved. A series of the energy feedback mechanisms were discussed also.
Chen and Zhao (2010) developed a thermodynamic model based on the MU model and coupled it to the upper ocean. Using this model the NSTM was numerically simulated and proved successful. The result is consistent with the observed results. It is verified that the solar radiation was the dominant energy source. Meanwhile, long-wave flux, air temperature, and atmospheric humidity play important roles in determining the relative intensity of NSTM. As the solar energy would be obstructed from thick ice, the NSTM is formed on the areas of thin ice, leads, and still open water.
In this study the thermodynamic coupled sea ice-upper ocean model (Chen and Zhao, 2010) is used to calculate the energy provided to the NSTM by solar radiation and the energy fed back to the sea ice.

2. SEA ICE-UPPER OCEAN COLUMN MODEL

2.1 Sea ice model

In this thermodynamic coupled sea ice-upper ocean column model the sea ice model was developed from Maycut and Untersteiner (1971). The thermal diffusion equation was the main equation as followed (Chen and Zhao, 2010),

$$\rho_i[c_0+\frac{L_0\mu S(z)}{T_i^2}]\frac{\partial T_i}{\partial t}=[k_0+\frac{\beta S(z)}{T_i}]\frac{\partial^2 T_i}{\partial z^2}+\kappa_i I_0\exp(-\kappa_i z) \quad (1)$$

Where, ρ_i is the sea ice density, T_i is the sea ice temperature, κ_i is the attenuation coefficient of short-wave radiation in sea ice, c_0 is heat

capacity of pure ice, k_0 is thermal conductivity of pure ice, L_0 is latent heat of pure ice at 0°C, μ and β are constants, S is salinity of sea ice which follow the parameterization scheme of the Los Alamos sea ice model (CICE 3.14, 2006), I_0 is the interior solar radiation penetrating the sea ice surface, and is expressed according to Beer's law combined with Bettge et al. (1996) method.

2.2 Ocean model

The vertical thermal diffusion equation is similar to the equation of the sea ice and expressed as followed,

$$\rho_w c_w \frac{\partial T_w}{\partial t} = \rho_w c_w \frac{\partial}{\partial z}\left(k_T(z)\frac{\partial T_w}{\partial z}\right) + \lambda(F_{pi} + F_{pl})\exp(-\mu h - \lambda z) \quad (2)$$

Where T_w is the temperature of sea water, ρ_w is the density of the sea water , c_w is the heat capacity of sea water, $k_T(z)$ is the turbulent diffusion coefficient of sea water, λ is the attenuation coefficient of sea water, F_{pi} and F_{pl} is the solar radiation penetrating the sea ice and the leads.

2.3 Precipitation

The prescribed precipitation was derived from climatological data (NCEP reanalysis2). The monthly data at the position (79°N, 140°W) in the Arctic was selected. Timely values were obtained by a cubic spline-interpolation through the monthly mean values.

Steele et al. (2004) found that there was a cold water at the depth of 150m in the Canada Basin. This water was stable and the maximum difference was 0.08°C (Shi et al., 2005). So the bottom boundary was fixed at the depth of 150m, and the temperature of the boundary was -1.5°C in this model.

The sea ice model was divided into 10 layers, and the ocean model was divided into 150 layers. The time step was 8 hours. The implicit time difference scheme was used here.

3. ANNUAL VARIATION OF SOLAR RADIATION FLUX AND OCEAN HEAT FLUX

Most of the solar radiation flux was reflected back into the atmosphere by the sea ice, part of it is absorbed by the sea ice, and the rest heats the surface sea water by penetrating through the sea ice. This part of solar radiation flux was the main heat source of the upper ocean (Maykut, 1995). At the same time the heat flux of the upper ocean transported heat to the sea ice.

The solar radiation flux penetrating through the sea ice was calculated as the following equation:

$$F_{top} = (1-\alpha_i)(1-i_0)F_{sw} + \varepsilon_i(F_{lw} - \sigma T_0^4) + F_{sens} + F_{lat} = -F_{c0} \quad (3)$$

Where, F_{sw} is the downward short-wave solar radiation, F_{lw} is the downward long-wave solar radiation, F_{sens} is the sensible heat flux, F_{lat} is the latent heat flux, F_{c0} is the surface heat transfer flux. And all of these fluxes are positive downward. α_i is the surface albedo of short-wave radiation, i_0 is the transmission coefficient of short-wave radiation, ε_i is the emission coefficient of long-wave radiation, σ is Stefan-Boltzman constant， T_0 is the surface temperature.

The heat flux at sea ice bottom absorbed from the sea F_{bi} is expressed as followed,

$$F_{bi} = 2\rho_w c_w k_T(z)(T_{w1} - T_{bi})/h_w \quad (4)$$

ρ_w and c_w are the same as above. T_{wl} is the upper seawater temperature. h_w is the thickness of one layer. The model is forced using the climate state value which was the same as Chen and Zhao (2010). And the parameters are shown at the end of this paper.

The solar radiation net flux and the sea ice bottom heat flux absorbed from the upper ocean are shown in Fig. 1. The solar radiation net flux penetrating through the sea ice was concentrated from June to September, and the maximum was 13 Wm^{-2} in the later July. In later June the ocean heat flux increases rapidly which was similar to the solar radiation net flux. The maximum appeared in August which was later than the solar radiation and the value is about 7 Wm^{-2}. After September the solar radiation net flux decreased to 0 rapidly but the ocean heat flux remained a little which indicates the role of energy saving of the ocean. The remained ocean heat flux existed till next year which indicated that the ocean might heat the sea ice in winter. The average of the solar radiation net flux (1.88 Wm^{-2}) was higher than the ocean heat flux (1.72 Wm^{-2}). So most of the heat flux of the solar radiation penetrating the sea ice was return to the sea ice and a little heat flux might transport to the deeper ocean.

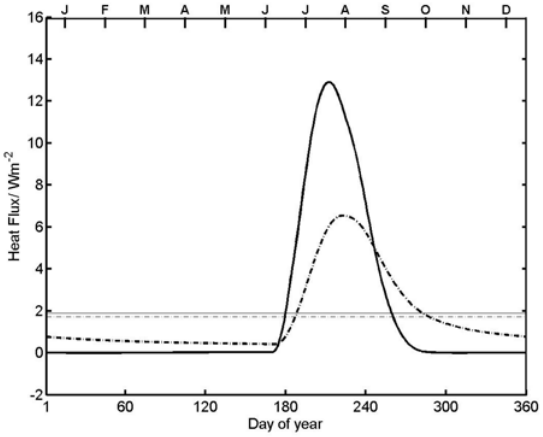

Fig 1. Annual cycle of the solar radiation net flux penetrating through the sea ice (thick solid line) and the upwards ocean heat flux at the bottom of the sea ice (thick dotted line). The thin solid line and the thin dotted line are the average of them.

4. THE RALATIONSHIP BETWEEN HEAT FLUX AND NSTM

4.1 Results of the observation data

The Ice Tethered Profiler (ITP) data deployed in the Canada Basin provide year-round observations from the upper water in the Canada Basin (Krishfield et al., 2008; Toole et al., 2006). Here, ITP3 and ITP4 data were examined to study the NSTM in 2006 (Fig 2). The locations of ITP4 were focused at 79°N, where the sea ice concentrations were

very high. The locations of ITP3 were southward relatively and the sea ice concentrations were lower than ITP4. There were some differences of the characteristic of the NSTM of these two data sets (Fig 4). The temperature maxima of the NSTM were higher when the sea ice concentration were lower, which was consistent with the studies of Cao et al. (2010). By changing the sea ice thickness (the sea ice concentration changed automatically in the model), the quantitative relationship between the solar radiation flux and the temperature maxima of the NSTM could be found and presented in the following section.

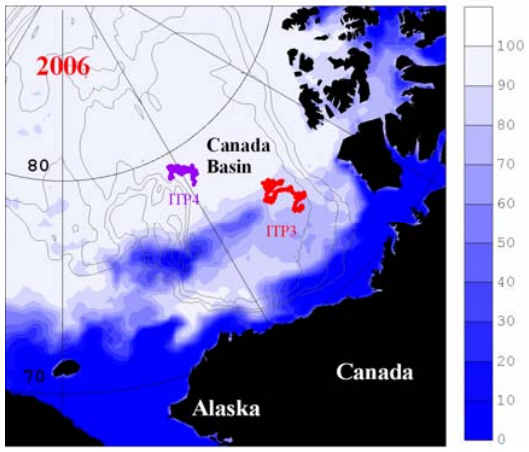

Fig 2. The locations of ITP3 and ITP4
The red dots indicate the location of ITP3 and the purple dots are the location of ITP4.The filled contour lines are the sea ice concentration at August in 2006 (0-100). The unfilled contour lines represent the topography.

Profile of temperature of ITP3 showed the vertical structure of the upper ocean in summer in 2006. The NSTMs were observed at the depth of 20db (Fig. 3). The temperature maximum of the NSTM were from -1.1°C to -0.7°C with the corresponding salinity less than 30. There was a temperature minimum water separated the Pacific Ocean inflow and the NSTM, which existed under the halocline corresponding to the NSTM peak.

Fig. 4 shows the variation of the temperature and the salinity of the

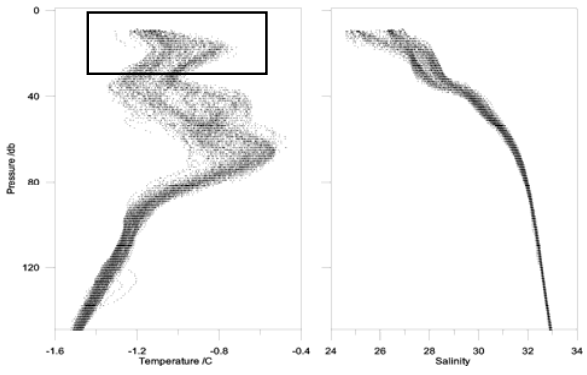

Fig 3. Profiles of temperature and salinity in summer (ITP3)
The temperature maximum in the black box indicated the NSTM

upper ocean (<150db) with the time. The temperature of the mixed layer began increasing from about 190d. The NSTM appeared at about 220d. So the time of the formation of NSTM is about 30 days. From November (310d) the temperature maximum of the NSTM became weaker until disappeared (The time was also depended by the location of the data).

4.2 The quantitative relationship between the heat flux and the NSTM

To simplify the model the atmospheric parameters at the central position in Arctic (79°N, 140°W) were used as the forcing values. The solar radiation flux was fixed at 328 Wm^{-2}. The long-wave radiation flux was fixed at 270Wm^{-2}. The air temperature was -2°C. The wind was 5ms^{-1}. The specific humidity is 2.8e-3$kgkg^{-1}$. The snow albedo α_s and the sea ice albedo α_i were fixed as 0.65 and 0.5 (Ebert et al., 1993). The initial conditions of the water temperature of all layers were -1.5°C. The observation data (fig 3 and fig 4) showed that the Pacific Ocean inflow at the depth of 50db-80db were more significant and persistent, whose temperature were higher than the NSTM. But for the existence of the pycnocline which was usually exist between the NSTM and the Pacific Ocean inflow, the vertical heated transport would be blocked partly. The influence of the Pacific Ocean inflow was omitted to simplify the model, which would be discussed in the later study.

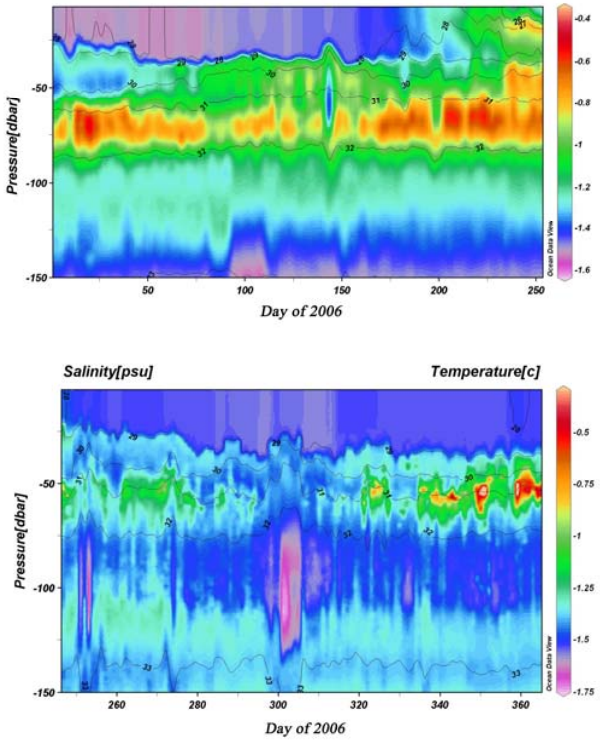

Fig 4. Results from ITP3 (up) and ITP4 (down)
The filled contour plot is temperature and the black lines indicate the salinity contours at 1 salinity unit intervals. The temperature maximum water in the black box indicated the NSTM.

$k_T(z)$ is an important parameter in the model. But it is complex under the sea ice and the study of it was few. Morison et al. (1985) found that $k_T(z)$ is much higher in the sea-surface layer (0-25m) than which in the deeper water. Zhang et al. (2007) calculated $k_T(z)$ by using the

data obtained from the 2nd Chinese National Arctic Research Expedition (CHINARE, 2003). The results showed that it was 1.0e-4 m^2s^{-1} in the surface layer and decreased to about 1.0e-5m^2s^{-1} in the depth from 25m to 60m, and then increased again. Without considering the influence of the Pacific Ocean inflow, the vertically varied eddy diffusivity was fitted by the observed temperature to simulate the typical sharp peak of NSTM. It was about 5.0e-3 m^2s^{-1} just under sea ice, whereas decreased down to 1.0e-6 m^2s^{-1} at the peak of the NSTM caused by the stratification of halocline (Chen and Zhao, 2010). Here we used the value as same as Chen and Zhao (2010). The results of the observation data (Fig 4) showed that the time of the formation of the NSTM was about 30 days. So the calculated time of the model was selected as 30 days also.

By changing the initial sea ice thickness from 4m to 0.15m, the different temperature maxima of the NSTM were modeled. When sea ice thickness is 4m, there is little solar radiation (about 2 percent) penetrate through the sea ice until the sea ice thickness decreasing to 1.5m. The heat fluxes were integral by calculating 30 days. Table 1 gives a quantitative relationship between the solar radiation net flux, the ocean heat flux on the bottom of the sea ice and the temperature maxima of the NSTM. Here the ocean heat flux respected the heat flux absorbed by the sea ice bottom. These results should be identified by the observation data. The solar energy through the sea ice to generate was from 10.90 Wm^{-2} to 45.30 Wm^{-2} corresponding the maximum temperature from -1.23°C to -0.39°C. The ocean heat flux was from 5.64 Wm^{-2} to 23.31 Wm^{-2}, which was about half of the solar radiation into the sea water. The results should be examined by the observation data.

Table 1. The relationship between the solar radiation net flux, the ocean heat flux and the maximum temperature of NSTM

T_{max} /°C	-1.23	-1.22	-1.21	-1.20	-1.19	-1.18	-1.17
F_{nets} / Wm^{-2}	10.90	11.26	11.64	12.05	12.49	12.85	13.22
F_{ice} /Wm^{-2}	5.64	5.83	6.03	6.24	6.47	6.65	6.85
T_{max} /°C	-1.16	-1.15	-1.14	-1.13	-1.12	-1.11	-1.10
F_{nets} / Wm^{-2}	13.61	14.03	14.47	14.78	15.27	15.61	15.98
F_{ice} /Wm^{-2}	7.05	7.26	7.49	7.65	7.91	8.09	8.27
T_{max} /°C	-1.09	-1.08	-1.07	-1.06	-1.05	-1.04	-1.03
F_{nets} / Wm^{-2}	16.35	16.75	17.16	17.60	18.05	18.29	18.78
F_{ice} /Wm^{-2}	8.47	8.67	8.89	9.11	9.35	9.47	9.72
T_{max} /°C	-1.02	-1.01	-1.00	-0.99	-0.98	-0.97	-0.96
F_{nets} / Wm^{-2}	19.04	19.57	19.85	20.43	20.73	21.04	21.36
F_{ice} /Wm^{-2}	9.86	10.13	10.27	10.57	10.73	10.89	11.05
T_{max} /°C	-0.95	-0.94	-0.93	-0.91	-0.90	-0.89	-0.88
F_{nets} / Wm^{-2}	21.69	22.37	22.73	23.28	23.66	24.06	24.47
F_{ice} /Wm^{-2}	11.22	11.58	11.76	12.05	12.25	12.45	12.66
T_{max} /°C	-0.87	-0.86	-0.85	-0.84	-0.83	-0.81	-0.80
F_{nets} / Wm^{-2}	24.89	25.33	25.78	26.25	26.74	27.24	27.76
F_{ice} /Wm^{-2}	12.88	13.11	13.34	13.58	13.84	14.09	14.36
T_{max} /°C	-0.79	-0.77	-0.76	-0.74	-0.73	-0.71	-0.69
F_{nets} / Wm^{-2}	28.31	28.87	29.45	30.06	30.69	31.36	32.04
F_{ice} /Wm^{-2}	14.64	14.93	15.23	15.55	15.87	16.21	16.56
T_{max} /°C	-0.67	-0.65	-0.63	-0.61	-0.59	-0.57	-0.54
F_{nets} / Wm^{-2}	32.77	33.52	34.30	35.13	35.99	36.92	37.88
F_{ice} /Wm^{-2}	16.94	17.32	17.73	18.15	18.59	19.07	19.56
T_{max} /°C	-0.52	-0.49	-0.46	-0.43	-0.39	-0.35	
F_{nets} / Wm^{-2}	38.91	40.01	41.17	42.43	43.79	45.30	
F_{ice} /Wm^{-2}	20.09	20.64	21.23	21.88	22.56	23.31	

5. CONCLUSIONS

A thermodynamic coupled sea ice-upper ocean column model was used in this paper to study the thermal feedback mechanism of Near Surface Temperature Maximum (NSTM).

The annual variation of the solar radiation flux and the ocean heat flux were studied in this paper that these two heat flux were concentrated from June to September. A part of ocean heat flux could remain till next year, which indicated the heat saving ability of the ocean. The average of the solar radiation net flux (1.88 Wm^{-2}) was higher than the ocean heat flux (1.72 Wm^{-2}). Most of the heat flux of the solar radiation penetrating the sea ice was return to the sea ice and a little heat flux might transport to the deeper ocean.

The solar radiation is the direct heat source of NSTM. With the simplified forcing field the model gave the quantitative relationship between the heat flux and the NSTM. The solar energy through the sea ice to generate was from 10.90Wm^{-2} to 45.30 Wm^{-2} corresponding the maximum temperature from -1.23°C to -0.39°C. The energy of sea ice obtained from NSTM was calculated also. The heat flux absorbed by the sea ice bottom was from 5.64 Wm^{-2} to 23.31 Wm^{-2}, which were half of the solar radiation flux.

ACKNOWLEDGEMENTS

Our thanks go to all the scientists and technicians who carried out ITP. This work is funded by National Natural Science Foundation of China (No. 40976111 and No. 40876003).

Appendix：Parameters in the model

ρ_w	Water density (kg m^{-3})	1024
ρ_i	Sea ice density (kg m^{-3})	917
c_w	Sea water specific heat (J kg^{-1} K^{-1})	3986.5
c_0	Pure ice specific heat (J kg^{-1} K^{-1})	2100
L_0	Pure ice latent heat (J kg^{-1})	3.34e5
L_b	Latent heat of ice bottom volume (Jm^{-3})	2.679e8
L_i	Latent heat of sea ice volume (Jm^{-3})	3.014e8
σ	Stefan-boltzman constant ($Wm^{-2}K^{-4}$)	5.67e-8
T_{i0}	Pure ice freezing point (°C)	0
T_{s0}	Pure snow freezing point (°C)	0
T_f	Sea ice freezing point (°C)	-1.5
κ_i	Attenuation coefficient of short-wave radiation in sea ice (m^{-1})	1.5
λ	Attenuation coefficient of sea water (m^{-1})	0.05
ε_i	emission coefficient of long-wave radiation	0.99
ε_w	Emission coefficient of sea water long-wave radiation	0.97
α_s	Snow surface albeso of short-wave radiation	0.65
α_i	Ice surface albedo of short-wave radiation	0.5
α_w	Sea surface albedo of short-wave radiation	0.1
i_0	transmission coefficient of short-wave radiation	0.17
β	Experiential constant ($Wm^{-1}psu^{-1}$)	0.117
μ	Experiential constant ($Kpsu^{-1}$)	0.054

REFERENCES

Bettge T W, J W Weatherly, W M Washington et al, 1996. The NCAR CSM sea ice model. Natl. Cent. for Atmos. Res., Boulder, Colo. Note: TN-425+ STR, 25 pp

Cao Y, Su J, Zhao J P, Li S J, Xu D (2010). "The Study on Near Surface Temperature Maximum in the Canada Basin for 2003-2008 in Response to Sea Ice Variations." Proceedings of the Twentieth (2010) International Offshore and Polar Engineering Conference, Beijing, China, ISOPE, Vol 1, www.isope.org.

Chen, ZH, Zhao, JP (2010). "Simulation for the thermodynamics of subsurface warm water in the Arctic Ocean," Acta Oceanologica and limnologica, Vol 41, No 2, pp 167-174. (in Chinese with English abstract)

Ebert E E, J A Curryy (1993). "An intermediate one dimensional thermodynamic sea ice model for investigating ice-atmosphere interactions". J Geophys Res, 98: 10085-10109

Jackson J M, Carmack E C, McLaughlin F A,Allen S E, Ingram R G, (2010). "Identification, characterization and change of the near-surface temperature maximum in the Canada Basin, 1993-2008." Journal Geophysical Research, in press.

Kadko D (2000). "Modeling the evolution of the Arctic mixed layer during the fall 1997 Surface Heat Budget of the Arctic Ocean (SHEBA) Project using measurements of 7Be." J Geophys Res，105(C2), pp 3369–3378.

Krishfield R, Toole J, Proshutinsky A and Timmermans M L (2008). "Automated Ice-Tethered Profilers for Seawater Observations under Pack Ice in All Seasons. " Journal of Atmosheric and Oceanic Technology, 25,11, pp 20912015

Maycut G A, Untersteiner (1971). "Some results from a time dependent thermodynamic model of sea ice." J Geophs Res, 76, pp 1550-1575.

Maycut G A, Mcphee M G (1995). "Solar heating of the Arctic mixed layer." J Geophys Res, 100, pp 24691-24703.

Morison J H, Long C E, Levine M D (1985). "Internal wave dissipation under sea ice," J Geophys Res, 90, pp 11959-11966.

Shi J X, Cao Y, Gao G P, et al, 2005. Distributions of Pacific-origin waters in Canada Basin in summer, 2003. Acta Oceanologica Sinica, 24(6), pp 12-24.

Steel M，Morion J, Ermold W et al, (2004). "Circulation of summer Pacific halocline water in the ArcticOcean." J Geophys Res, 109, C02027, doi: 10 1029/2003JC002009.

Toole J, Krishfield R, Proshutinsky A, Ashjian C, Doherty K, Frye D, Hammar T, Kemp J, D. Peters, Timmermans M L, Heydt K, Packard G and Shanahan T (2006). "Ice Tethered-Profilers Sample the Upper Arctic Ocean" EOS, Transactions of the American Geophysical Union, 87, 41, pp 434-438.

Zhang Ying, Zhao Jinping (2007). "The Estimation of Vertical Turbulent Diffusivity in the Surface Layer in the Canada Basin," Periodical of Ocean University of China, 37, 5, pp 695-703.

Zhao, J P, Shi, J X, Jiao, Y T (2003). "Temperature and salinity structure in summer marginal ice zone of Arctic Ocean and an analytical study on its thermodynamics, " Acta Oceanologica and limnologica, 34(4), pp 375-388. (in Chinese with English abstract)